Guntram Rüf, Christof Sommitsch and Bruno Buchmayr:

Modelling ductile damage of a Ni-base alloy considering the microstructure evolution during hot working

Macro- and microscopically based continuum damage failure criteria as well as the model of effective stresses (MES) are validated for a nickel-base alloy by means of an experimental database from hot compression tests. Most models show maximum damage for cylindrical specimens at the experimentally determined fracture site but do not predict the correct fracture site for collar test specimens with adequate precision. For all models excepting the MES, a lack of transferability of critical values to different testing conditions can be determined.
Additionally, a semi-empirical grain structure model is coupled to the damage evolution in order to describe the influence of materials' softening by dynamic recrystallization on lifetime consumption. With the onset of recrystallization the accumulated deformation, i. e. the effective plastic strain is reduced by recrystallization and hence the damage evolution rate is decreased. EBSD analyses of hot deformed samples are performed to validate the model and to investigate the interaction of crack initiation as well as of crack progress with dynamic recrystallization.

To meet the requirements that modern product designs and properties make on manufacturing processes, especially in the range of forming technologies, computer aided design and manufacturing methods have to be applied. Hence it is necessary to understand forming processes with respect to the influence of main process parameters, e. g. temperature, geometries, deformation rate, friction and loading rates on the process limitations. Ductile failure of material, which could be defined as crack initiation is, apart from folding, necking or surface roughening, one of the most important limiting factors in forming processes [1; 2]. To achieve a continuous simulation chain within the scope of a virtual manufacturing approach, the description of material damage becomes more important to ensure safe manufacturing processes in bulk hot forming even at the forming limits of metals. Severely deformable materials often exhibit very close deformation windows regarding temperature and deformation rate, in particular during bulk hot forming as well as with multi-pass deformation processes. In order to remain in these optimal forming windows, the continuum-mechanical modelling of damage should be able to predict materials failure independent of geometries, depending only on the material.

Within this article continuum-mechanical either empirical or micro-mechanical based damage models are evaluated by means of numerical finite element (FE) simulation and experiments with regard to their applicability for predicting failure of the nickel-base alloy 80A in the critical temperature range between 900 and 1000 °C. By coupling a semi-empirical microstructure model with lifetime consumption, the influence of dynamic recrystallization on the damage evolution is investigated.

Damage models

Integral formulation. One limiting factor in metal forming is crack initiation due to severe plastic deformation. Metallurgical investigations showed that micromechanically ductile failure is characterized by void nucleation at inclusions, second-phase particles or grain boundaries, by void growth and by coalescence of voids. The first coalescence of voids is defined as crack initiation and is followed by crack growth [3; 4].

These processes depend upon parameters like stress state, strain, strain rate, friction and forming temperature [2].

Therefore many researchers tried to formulate damage criteria to predict ductile failure in forming processes. Most models can be written in the generalized form

Table 1: Investigated damage criteria. $\bar{\sigma}$ is the equivalent stress, $\bar{\varepsilon}$ is the equivalent strain, σ_{max} is the maximum principal stress, $\sigma_{i,j}$ are principal stresses, n is the hardening coefficient, a is a weighting factor for the stress triaxiality, $\sigma_{m,H}$ is the hydrostatic stress, σ_u is the ultimate tensile strength and $\bar{\varepsilon}_f$ is the equivalent fracture strain

Freudenthal [8]	$C = \int_0^{\bar{\varepsilon}_f} \bar{\sigma} d\bar{\varepsilon}$
Normalized Cockcroft & Latham [9]	$C = \int_0^{\bar{\varepsilon}_f} \frac{\sigma_{max}}{\bar{\sigma}} d\bar{\varepsilon}$
Cockcroft & Latham [10]	$C = \int_0^{\bar{\varepsilon}_f} \sigma_{max} d\bar{\varepsilon}$
McClintock [11]	$C = \int_0^{\bar{\varepsilon}_f} \left[\frac{\sqrt{3}}{2 \cdot (1-n)} \sinh\left(\frac{\sqrt{3}(1-n)}{2} - \frac{\sigma_i + \sigma_j}{\bar{\sigma}} \right) + \frac{3}{4} \frac{\sigma_i - \sigma_j}{\bar{\sigma}} \right] d\bar{\varepsilon}$
Rice & Tracey [12]	$C = \int_0^{\bar{\varepsilon}_f} \exp\left(\frac{\alpha \sigma_m}{\bar{\sigma}} \right) d\bar{\varepsilon}$
Oyane [13]	$C = \int_0^{\bar{\varepsilon}_f} \left[1 + \frac{1}{a_0} \frac{\sigma_m}{\bar{\sigma}} \right] d\bar{\varepsilon}$
Ayada [14]	$C = \int_0^{\bar{\varepsilon}_f} \frac{\sigma_m}{\bar{\sigma}} d\bar{\varepsilon}$
Brozzo [15]	$C = \int_0^{\bar{\varepsilon}_f} \left(\frac{2\sigma_{max}}{3(\sigma_{max} - \sigma_H)} \right) d\bar{\varepsilon}$
Zhao & Kuhn [16]	$C = \frac{\sigma_{max} \bar{\varepsilon}}{\bar{\sigma}}$
max. princ. stress / ultimate tensile strength, (MPUT)	$C = \frac{\sigma_{max}}{\sigma_u}$

$$C = \int_0^{\bar{\varepsilon}_f} f(\text{stress state})\, d\varepsilon_{eq}\,, \qquad (1)$$

where C denotes a parameter, which could be interpreted as the critical value when failure occurs. f is a function of the stress state and the deformation history, respectively, which is integrated by the equivalent strain, with the failure strain $\bar{\varepsilon}_f$ as upper boundary, and can include more parameters [5].

The main aim of damage modelling is to predict the correct failure sites, independent of geometry, deformation history, deformation rates and temperature. Therefore critical values should be material constants [6].

Generally, damage modelling can be separated into a phenomenological (macro-mechanical) and a micro-mechanical approach considering void growth theory [3; 4; 6; 7].

In **table 1** damage models used in this article are shown. Most of these models are so-called one parameter criteria, which calculate an accumulated damage value that can be denoted as the critical value at the fracture strain. But models like Rice & Tracey, McClintock, Oyane and MPUT use an additional material dependent parameter that can be adapted inside reasonable limits for a better correlation of numerical and experimental results as well as for the applicability in a broader range of process conditions.

The parameter n in the McClintock criterion denotes the hardening coefficient, which was determined by hot tensile tests [3; 4; 9]. For the examined temperature range, the values 0.045 (900 °C), 0.046 (950 °C) and 0.0326 (1000 °C) were obtained. In the model of Rice & Tracey the factor α can be used as a weighting factor for the influence of the stress triaxiality on the void growth [1; 3]. However, adjustments of this factor are not recommendable, because they challenge the mechanical well-founded derivation of the model [3]. Therefore the original factor of 1.5 was taken for the simulations [12]. The parameter a_0 in the Oyane model can be derived by experiments with two different stress states by an approximation of the experimental results through the linear equation implied in the model [13; 17]. In this case the temperature dependence of the parameter was investigated and it was determined by the results of the experiments performed on specimens with a height to diameter ratio of 2 : 1 to a value of 0.2444. In comparison the value of 0.4 taken from literature and determined by K. Osakada and H. Hayashi [13] in tension and compression tests on malleable cast iron was used for the numerical simulations. The ultimate tensile strength σ_u necessary for the MPUT model was also obtained from hot tensile tests in the critical temperature range of 900 °C (σ_u = 218 MPa), 950 °C (σ_u = 135 MPa) and 1000 °C (σ_u = 79 MPa).

Model of effective stresses. Alternatively to the above mentioned criteria an isotropic continuum damage model by Lemaitre based on the concept of effective stresses (MES), which is derived within a thermo-dynamical framework was used to predict ductile damage [18]. Dividing the material into representative volume elements, it is assumed that with the occurrence of a damage D by formation of pores only the fraction 1-D of the section of a volume element carries the applied loads. All parameters affected by ductile failure are accordingly treated as effective values. For the effective stress tensor $\tilde{\bar{\sigma}}$ thus follows [19; 20]:

$$\tilde{\bar{\sigma}} = \frac{\bar{\sigma}}{1-D}\,, \qquad (2)$$

where $\bar{\sigma}$ is the Cauchy stress tensor and D is $\tilde{A}/A_0$. $\tilde{A}$ is the area of pores in the section and A_0 is the original area.

The law of evolution of damage derives from the potential of dissipation Ψ, which is a scalar convex function of the state variables in case of isotropic plasticity and isotropic damage [18; 19]:

$$\dot{D} = -\frac{\partial \Psi}{\partial Y} = \left(\frac{Y}{S_0}\right)^{s_0} \dot{\bar{\varepsilon}}\,, \qquad (3)$$

where S_0 and s_0 are material and temperature dependent and $\dot{\bar{\varepsilon}}$ is the equivalent true strain rate.

The damage energy release rate Y corresponds to the variation of internal energy density due to damage growth at constant stress. As a main deviation to the standard model in these investigations the enhanced model of Lemaitre was used, where the stress tensor was split into a positive and a negative part, to distinguish between tensile and compressive stresses in a multi-axially stressed state [19; 21]:

$$Y = \frac{1+n}{2E}\left[\frac{\langle\bar{\sigma}\rangle:\langle\bar{\sigma}\rangle}{(1-D)^2} + \frac{h\ \langle-\bar{\sigma}\rangle:\langle-\bar{\sigma}\rangle}{(1-hD)^2}\right] + \frac{n}{E}\left[\left(\frac{\mathrm{tr}(\langle\bar{\sigma}\rangle)}{1-D}\right)^2 + h\ \left(\frac{\mathrm{tr}(\langle-\bar{\sigma}\rangle)}{1-hD}\right)^2\right] \qquad (4)$$

where h is a crack closing parameter [19; 21], which describes the effect of partial microcrack/void closure under a compressive stress state, $\mathrm{tr}(\bar{\mathbf{x}})$ denotes the trace of a tensor and $\langle\mathbf{x}\rangle$ is the Macauley bracket:

$$\langle\mathbf{x}\rangle = x \quad \text{if} \quad x \geq 0,$$
$$\langle\mathbf{x}\rangle = 0 \quad \text{if} \quad x < 0\,. \qquad (5)$$

The crack closure parameter h has to be chosen very small ($h \sim 0$) to get the maximum damage in the barrelling zone with maximum circumferential tension stresses. In this region, cracks were detected first experimentally. Larger values for h lead to calculated crack occurrence at the edge of the specimen due to very high strains and compressive stresses there.

For the prediction of the material parameter, tensile tests of alloy 80A were carried out for different temperatures between 900 °C and 1000 °C. In this temperature range, carbides and γ' particles precipitate and thus decrease the hot formability drastically. According to Lemaitre [19], S_0 can be derived from the tensile test by:

$$S_0 = \frac{\sigma^2}{2E(1-D)^2\,\frac{dD}{d\varepsilon}}\,. \qquad (6)$$

If we assume $\partial D / \partial \varepsilon$ as sufficiently linear [18; 19] given by:

$$\frac{\partial D}{\partial \varepsilon} \approx \frac{\Delta D}{\Delta \varepsilon} = \frac{D_{1c}}{\varepsilon^{p}_{rupture}}, \quad (7)$$

S_0 can be derived by inserting the flow stress to rupture σ_R for σ and D_{1c} for D in eq. (6). $\varepsilon^{p}_{rupture}$ denotes the elongation at rupture and D_{1c} is the critical damage in the uniaxial tension test that is given by [19]:

$$D_{1c} = 1 - \frac{\sigma_R}{\sigma_u}, \quad (8)$$

with σ_u as the ultimate tensile strength.

The rupture criterion D_c can be derived by

$$D_c = D_{1c} \frac{\sigma_u^2}{\sigma_{eq}^2 R_v} \leq 1, \quad (9)$$

with σ_{eq} as the equivalent stress and R_v as a function of stress triaxiality [18; 19]. The quotient σ_u/σ_{eq} depends not only on temperature but also on the strain rate in the high temperature regime.

The evolution of damage was calculated by

$$D_i = D_{i-1} + \frac{\dot{D}\,\Delta t}{D_c}, \quad (10)$$

where i demarks the time step. Hence rupture is assumed if D_i equals 1.

Microstructure model

The softening process in materials with a relatively low stacking fault energy, e. g. steels in the austenitic regime, copper or nickel-base superalloys, is mainly governed by

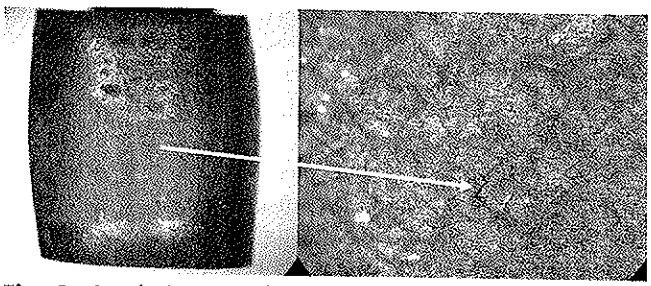

Fig. 1: Crack detection for a specimen compressed at a testing temperature of 900 °C, alloy 80A

recrystallization. After reaching a critical strain during deformation, the nucleation and growth of recrystallization grains start. These new, initially stress free grains experience deformation during the ongoing hot deformation and thus can lead to a further recrystallization cycle [22]. The strain ε_p at maximum flow stress σ_p is given by [23] $\varepsilon_p = A\, d_0^{l}\, Z^{m}$, with A, l, m as constants, d_0 as the initial mean grain size and Z as the Zener-Hollomon parameter. The critical strain for the initiation of dynamic recrystallization can be set into relation to the peak strain by $\varepsilon_c = k_c\, \varepsilon_p$, where the constant k_c has typical values of 0.60 - 0.86 [23]. The time for 50 % dynamic recrystallization is calculated by $t_{0.5} = B Z^{-b} (Q_{def}/RT)$, where B, b are constants, Q_{def} is the activation energy for deformation, R is the gas constant and T is the temperature. Inserting $t_{0.5}$ into the Avrami type equation for the recrystallized fraction $X = 1 - \exp\left[(-\ln 2)\cdot(t/t_{0.5})^{k}\right]$ delivers the dynamically recrystallized (DRX) fraction X_{dyn}

$$X_{dyn} = 1 + \exp\left\{-0.693 \cdot \left[\frac{t \cdot Z^{b}}{B^{k}} \cdot \exp\left(-\frac{Q_{def}}{RT}\right)\right]^{k}\right\}, \quad (11)$$

with B, b as well as k as material parameters. For the investigated alloy 80A, two temperature regimes with the critical temperature of 1020 °C have to be stated. The separation into two temperature regimes is necessary in order to account for the precipitation of carbides and the γ'-phase $Ni_3(Al,Ti)$ in the lower temperature regime [22].

Both models, described above, were implemented into the FE program Deform 2D with Lagrange code. The evolution of damage as a function of the dynamically recrystallized fraction was calculated by

$$D_i = D_{i-1} + \frac{\dot{D}\,\Delta t}{D_c}\left(1 - X_{dyn}\right), \quad (12)$$

where i indicates the time step, Δt the time increment and D_c the rupture criterion. Therefore rupture is assumed if D_i equals 1. If we reach a fully recrystallized structure, i. e. $X_{dyn} = 1$, the progress of material damage stops.

Experimental method

To evaluate the effectiveness and applicability of fracture criteria at elevated temperatures, tests with different starting temperatures had to be performed to consider metallurgical effects. One of the most commonly used tests for modelling forging processes and for studying the location and moment when failure occurs is the uniaxial hot compression test of a cylindrical specimen between flat plates [24]. Because of the friction between the specimens and the tools a barrelling effect occurs during the experiments on the surface near the horizontal symmetry section of the sample. The resulting circumferential stresses cause specimens to fracture [5; 25].

The failure initiation site and the resulting height when failure starts were detected by a nesting procedure. For each test condition a trial test was carried out with an upsetting rate of 50 % of the initial sample height. Depending on whether crack initiation has occurred or not the compression rate for the next test was reduced or increased until a crack with a length of approx. 0.1 mm was detected by means of a stereo microscope, **fig. 1**.

Testing facility and material. As material for the experimental investigations the nickel basis alloy 80 A with the following mass contents in %: 0.05 C; 1.67 Al; 0.15 Si;

2.52 Ti; 19.60 Cr; 0.04 Mn; 0.06 Co; 0.03 Mo; Ni-bal. was used.

The cylindrical specimens with a height to diameter ratio of 1.5 : 1 and 2 : 1 were machined by turning from as hot-rolled rods of 35 mm diameter to an initial height of 24 mm or 32 mm and a diameter of 16 mm. Collar test samples had a height of 24 mm and a diameter of 16 mm as well as 22 mm at the collar, respectively. The collar was manufactured to a height of 8 mm.

The compression tests were conducted on a 100 t hydraulic press with open-loop control, a maximum die speed of 7 mm/s and a PC-based data acquisition system (Labview-tool) to get the data of die distance, time, force and specimen temperature. The upper die speed was constant during the tests and differed between 5.1 (1.5 : 1, 900 °C) and 6.8 mm/s (2 : 1, 1000 °C), depending on the various testing conditions.

The samples were heated by an inductive heating equipment controlled by a pyrometer after a predefined temperature cycle, including the heating up to a temperature of 1200 °C, 2 min holding time at an annealing temperature of 1200 °C and cooling down to the test temperature with a cooling rate of at least 5 K/s. The experiments were carried out with no lubrication between the work piece and the tools at temperatures of 900 °C, 950 °C and 1000 °C. The tools also were heated inductively and, as was shown by measurement, reached the same temperatures as the specimens. Due to this it was possible to obtain nearly isothermal conditions. The temperature of the samples was measured by thermocouples, which were located at the equatorial surface and additionally near the top and the bottom surface to determine deviations of sample and intended testing temperature.

Table 2: Values of geometry, temperature, die speed, maximum force and final height for selected specimens of alloy 80A

Geometry		mm	Temperature °C	Die speed, mm/s	Max. force, kN	Final height mm
1.5:1			900	5.1	131.5	20.3
	Height	24	950	6.2	85.4	15.9
	Diameter	16	1000	6.7	77.9	13.7
			1050	5.8		
			1100	5.8		
			1150	6		
2:1			900	6.2	133.21	19.1
	Height	32	950	6.7	104.5	16.8
	Diameter	16	1000	6.8	130.6	11.9
Collar test			900	5.1	157.14	22.1
	Height	24	950	5.6	98.82	17.7
	Diameter	16	1000	6	66.1	17.4
	Height collar	8				
	Diameter collar	22				
					Cracks detected	

Results

All samples showed crack initiation near the equatorial area of the surface. For the validation of the failure criteria those specimens were selected with the best correlation of sample temperature and target testing temperature and a minimum temperature gradient in the direction of the cylinder axis. Values of die speed, maximum force, geometry, temperature as well as final sample heights when failure starts, obtained from experiments are depicted in **table 2**. No cracks occurred at samples compressed at temperatures higher than 1000 °C.

Finite element model

The numerical simulations of the compression tests were carried out by using the commercial FE-code Deform 2D.

An axisymmetric non-isothermal model was built up representing one half of the testing facility and considering heat transfer. The tools, tool holders and ground plates were modelled as rigid surfaces. Due to earlier measurements, tools and work piece were set to the same values of temperature as the applied testing temperature. A surface-to-surface contact with friction was introduced to model the interactions between the tools and the specimen. Downward velocities for upper tool, tool holder and ground plate were defined analogous to measured values while the bottom ones were fixed. A boundary condition considering heat exchange with the environment was applied to all parts of the model.

The friction coefficient between the tools and the specimen was verified by the comparison of the experimental and the numerical results. A friction coefficient of 0.7 (shear) gave a good correlation with experiments in terms of the force-displacement response and the barrelling geometry obtained from the deformed samples. Stress-strain data provided by Böhler Edelstahl GmbH were used as material input to the isotropic plastic model (J2 plasticity). Simulation was stopped when the maximum force acquired from the experiment was reached.

A necessary condition to get an excellent simulation was an adequate correlation of force-displacement curves and the final height of the specimens for experiment and simulation. This is shown in **fig. 2** for specimens with a height to diameter ratio of 1.5 : 1. For other geometries very small deviations in curve progression between experiment and numerical simulation were also determined.

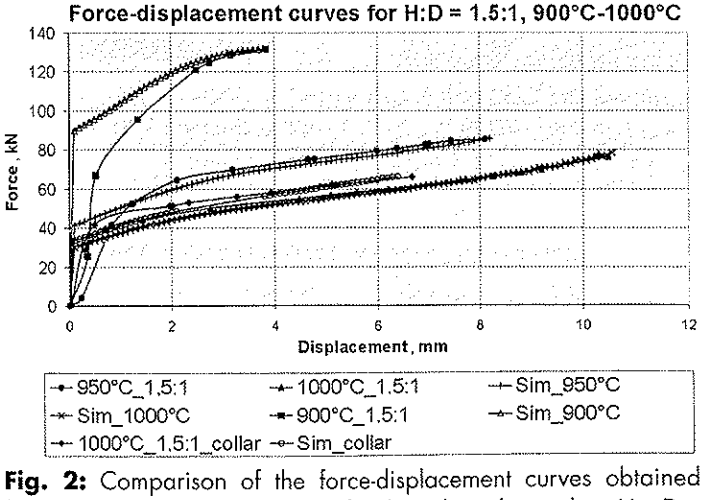

Fig. 2: Comparison of the force-displacement curves obtained from simulation and experiment for the selected samples, $H : D = 1.5 : 1$, alloy 80A

Critical damage values and damage prediction

A precondition for a practicable use of damage prediction by means of numerical simulation in industrial applications is that models should predict the correct fracture site independent of stress and strain history, strain rate, geometry and, within the scope of hot forming processes, independent of temperature as well. Model parameters should only depend on material and not on testing conditions and it should also be possible to determine parameters with simple standard tests. This implies that calculated critical values have to be material constants, if the identification of the model parameters was made correctly.

Therefore, deviations of critical values of the selected damage models have to be determined in order to analyze influences on process conditions (e. g. stress state, temperature).

To evaluate the precision in prediction of the fracture site by numerical simulation in comparison to the experimental results and to determine critical values of the selected damage models, those elements of the FE-mesh were selected, which showed the maximum damage values at the end of the simulation. Selected results up to this point are shown in **fig. 3**. For cylindrical specimens all models excepting Zhao & Kuhn and Freudenthal predicted for all temperatures the fracture site on the surface of the equatorial area of the sample as it could be expected from theoretical considerations as well as experiments showed. Freudenthal and Zhao & Kuhn showed maximum damage at the outer radius of the contact surface between tools and sample.

For collar test specimens all failure criteria excepting the Freudenthal model calculated maximum damage in contrast to experimental results in the transition of the cylindrical area to the collar. However, these models also indicated high values of damage at the surface in the equatorial area of the collar. Deviations lie between 9 % (McClintock) and almost 30 % (Zhao & Kuhn), depending on the model. The MES shows a maximum damage of 1 at the transition of the collar as well as at the equatorial surface.

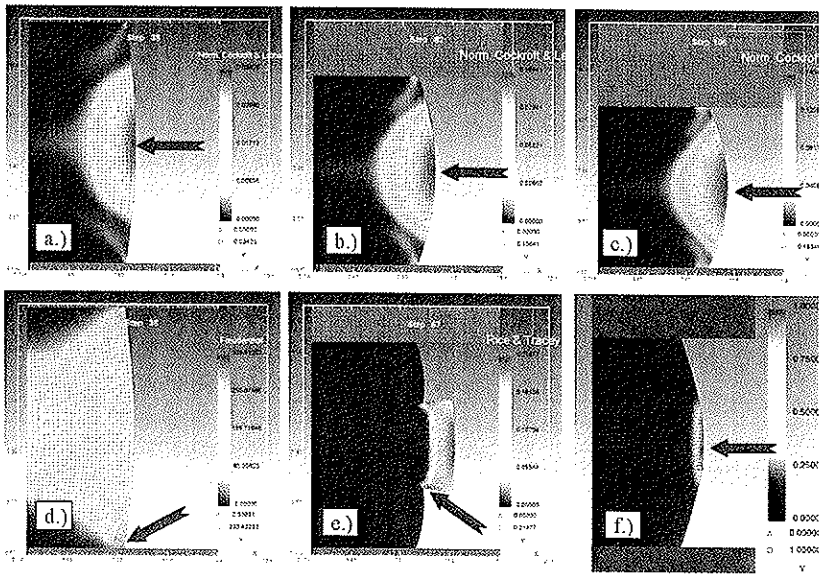

Fig. 3: Prediction of fracture site for selected damage models and various testing conditions, alloy 80A

a) normalized Cockcroft & Latham (NCL), 900 °C, 1.5 : 1; b) NCL, 950 °C, 1.5 : 1; c) NCL, 1000 °C, 1.5 : 1; d) Freudenthal, 900 °C, 1.5 : 1; e) Rice & Tracey, 950 °C, 1.5 : 1 collar test; f) MES, 1000 °C, 2 : 1

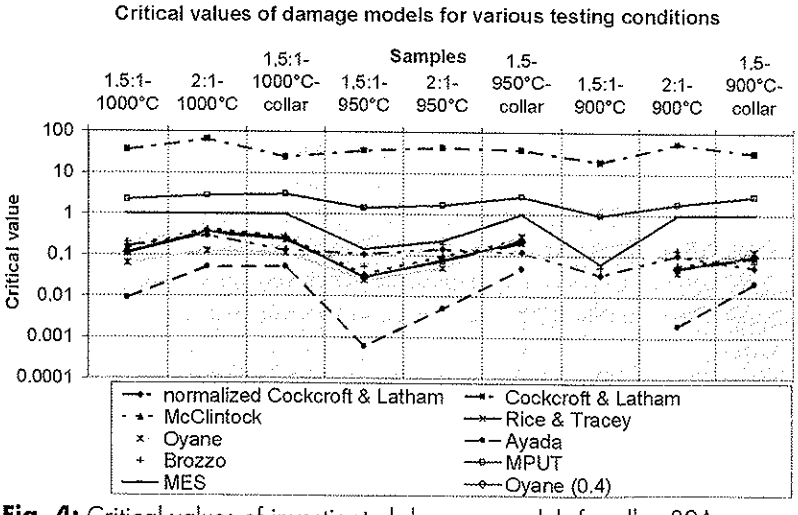

Fig. 4: Critical values of investigated damage models for alloy 80A

The results of the critical damage values for each failure criterion are shown in **fig. 4**. The models of Freudenthal and Zhao & Kuhn are not considered for further examinations due to their lack of accuracy in prediction of the correct failure location. Although the critical values should be material constants, it can be seen from fig. 4 that they are very different depending on the testing conditions.

Criteria like McClintock, Rice & Tracey, Ayada and Oyane which mostly are developed for high stress triaxialities and for the growth of voids, respectively, can not be applied for the prediction of failure in the range of negative hydrostatic stress, since this would cause shrinkage of the voids. In numerical calculations, the integrals are only evaluated for positive hydrostatic stress. Because of a negative stress triaxiality at the fracture location at a temperature of 900 °C and a $H : D$ ratio of 1.5 : 1, no damage value unlike zero was obtained for the above mentioned models (fig. 4).

Hence critical parameters did not only differ depending on testing geometry but also depending on testing temperature. E. g. for the model of McClintock, the value obtained at 950 °C for a 1.5 : 1 specimen was more than ten times smaller than the corresponding value at 1000 °C for a 2 : 1 sample and more than three times smaller than the analogous value at 1000 °C for a 1.5 : 1 specimen. The model of Ayada showed very small deviations in the comparison of the collar test and the 2 : 1 specimens at 1000 °C due to a very similar integral area in the triaxiality and the effective strain space, **fig. 5**. A comparable behaviour was observed for the Brozzo criterion in the temperature range of 900 °C to 950 °C for the 1.5 : 1 testing geometry, where very small deviations also occurred. There-

fore it can be conjectured that critical damage values of the previously described models can only be used for damage prediction within a small range of temperatures or stress state.

Generally, a good correlation of critical values was obtained for the MES model, although in some cases the damage evolution was both underestimated (1.5 : 1 and 2 : 1, 950 °C and 1.5 : 1, 900 °C) and overestimated (2 : 1, 1000 °C and 900 °C as well as for collar test at 900 °C to 1000 °C). However, these deviations are lower than 25 % comparing the experimental die displacement at fracture with calculations when the relative damage D_i reaches its critical value of 1. Only the testing condition of 900 °C for 1.5 : 1 showed larger deviations. Here, an absolute difference in distance means higher deviations because of the smaller die distances to fracture in comparison to tests at higher temperatures and/or larger $H : D$ ratios.

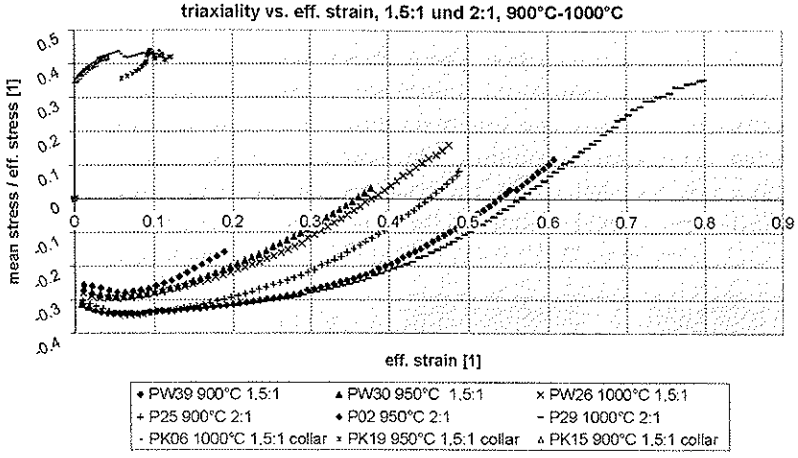

Fig. 5: Triaxiality vs. equivalent strain for various testing conditions

Deform 2D offers the possibility to analyze the stress-strain history during deformation of certain points by a point tracking function. Fig. 5 depicts the progression of triaxiality vs. the effective strain. On the one hand, at 900 °C and for a geometry of 1.5 : 1, failure occurs at a negative hydrostatic stress state whereas on the other hand, triaxiality is always positive at failure in the collar test throughout deformation.

Only for the MES, a comparability of calculated critical damage values is possible because reaching the value 1 of the relative damage parameter D_i defines the critical state of materials failure.

Consideration of materials softening in damage calculations

Various temperatures and strain rates cause differences of material microstructure that can not be covered by conventional micro- and macro-mechanical damage models. Therefore these models should only be compared for different stress states.

In hot forming processes, a regeneration of material formability by changes of microstructure due to dynamic recrystallization (DRX) takes place, which has to be considered in damage calculations at sufficiently high temperatures for softening processes. The deformation energy is reduced by the nucleation of initially undeformed grains. Therefore the damage rate and thus the possibility of crack initiation is diminished.

During hot compression, the maximum strain typically accumulates in the centre of the specimen as well as in the 45° direction related to the global load. Therefore the heat that develops during deformation leads to a temperature gradient between the centre and the edge of the specimen. Hence, the highest DRX fractions can be found in the areas of both maximum strain rate and temperature, **fig. 6**. With the onset of DRX the deformation strain is reduced and the grain triple points, critical for crack initiation, are removed by the progress of new DRX grains. Thus at steady state DRX, damage diminishes, even to zero. This is typically found for industrial hot forming applications at approx. 1050 to 1200 °C, moderate strain rates below 10 s^{-1} and compressive stresses for the investigated alloy 80A [22].

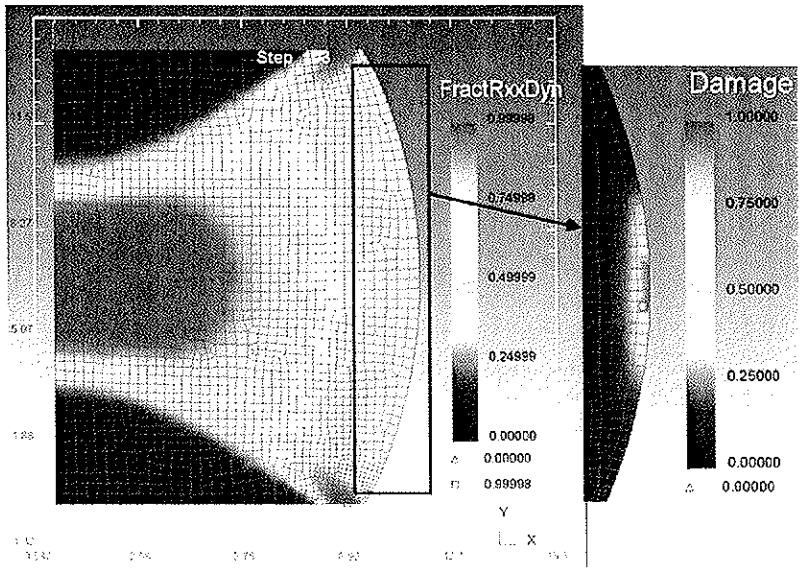

Fig. 6: Simulation of the dynamically recrystallized fraction at 1000 °C at the first appearance of macro cracks for alloy 80A. The accumulated damage (i. e. lifetime consumption) in the barrelling zone where the first macro cracks appear is zoomed out

For the EBSD (electron backscatter diffraction) measurements and analyses, an EDAX / TSL system attached to a scanning electron microscope was used. The OIM (orientation imaging microscopy)-maps show that with decreasing temperature the fraction of recrystallized grains also strongly decreases. For a temperature of 1000 °C it changes from approximately 40 % at 2/3 of the radius (70 % in the simulation) to 25 % at the edge of the specimen (30 % in the simulation). The measured DRX grain size was approx. 12 µm (calculations: 18 µm) at 2/3 of the radius and approx. 11 µm at the edge of the specimen (16 µm

in the simulations). For 900 °C only a few recrystallized grains can be observed, **fig. 7**. The grain orientation spread was used to discriminate between the original and the recrystallized grains [26]. For the unrecrystallized grains, contrarily to the recrystallized grains, a texture can be observed, which increases with increasing strain [27].

Microstructure was considered in damage calculations for cylindrical specimens ($H : D = 1.5 : 1$) in the temperature range of 900 °C to 1000 °C. In the low temperature regime of 900 °C it was not possible to determine an influence of microstructure on damage, whereas at temperatures of 950 °C and 1000 °C a reduction of damage rate was obtained, which leads to an adjustment of the parameter s_0 in eq. (3) in contrast to calculations without the microstructure model. This effect becomes obvious comparing transverse cross-sections in fig. 7 that show recrystallized grains for 1000 °C.

Crack initialization usually takes place at the triple points of the unrecrystallized grains where high stresses exist, especially near the edge of the sample with circumferential tensile stress components. However, crack propagation itself seems to depend on the degree of recrystallization. In samples with a rather high fraction of recrystallized grains the crack preferentially grows within the recrystallized region, not only along grain boundaries (fig. 7). This is a sign that at least part of the dynamic recrystallization has taken place before the crack formation.

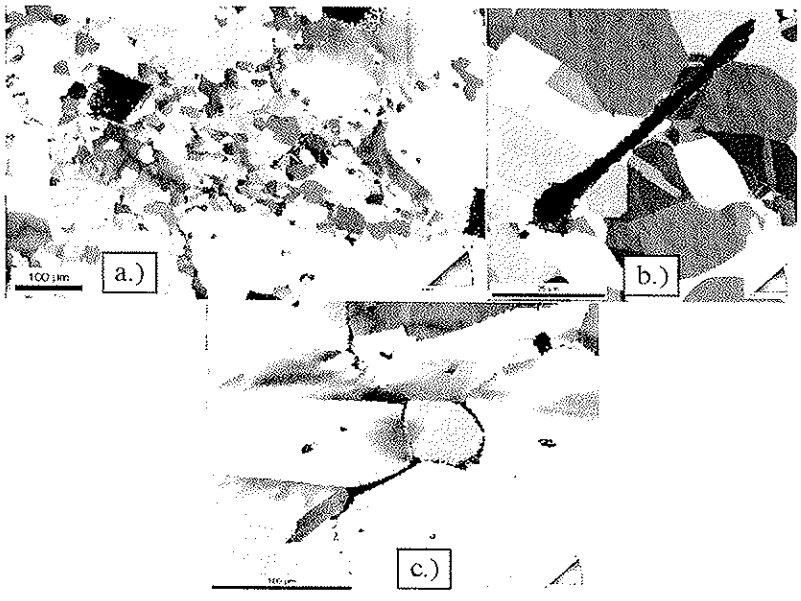

Fig. 7: OIM figures at a transversal cross-section of a compression specimen at 2/3 of the radius

a) T = 1000 °C, bar length: 100 µm; b) zoom from image a) with crack, bar length: 35 µm; c) T = 900 °C, bar length: 100 µm

inset in all figures: orientation triangle with grey code for crystal orientations; the black regions in fig. 7a result from micro-indentations made after the compression test

Even if only small clusters of recrystallized grains are present, the crack is connected to these clusters, which often confines the crack to a part of a grain boundary. Contrarily, in case of samples with a negligible amount of recrystallization during compression, the crack propagates along the grain boundaries of the deformed grains, tearing apart the grains, often singling out individual grains.

Summary

Macro- and microscopically based continuum damage failure criteria as well as the model of effective stresses were validated for the nickel-base alloy 80A for different testing conditions and sample geometries representing varying stress states. It was shown that the application of various damage models in numerical simulation provides the possibility to identify local failure correctly. However, the two damage criteria of Freudenthal and Zhao & Kuhn failed in predicting the correct fracture site for the applied testing conditions on cylindrical specimens.

Critical values of damage parameters could not be denoted as material constants. Only for some specific conditions and models, an adequate experimental correlation of damage parameters at failure could be reached. With a negative hydrostatic stress at failure location, the models of Oyane, Rice & Tracey, McClintock and Ayada are not applicable. As a consequence for industrial applications, critical damage values would have to be determined for each testing condition, which would cause an intensive experimental effort. Nevertheless, the transferability of experimental results to the numerical simulation of structural components is questionable, because critical damage parameters did not show an adequate correlation between experiments and simulations even in a small range of triaxiality and temperature.

A change in the stress state, achieved by collar tests, showed other failure limits than with the cylindrical samples for most of the selected damage models. However, it was possible to qualitatively identify the correct areas of damage excepting the model of Freudenthal, where the failure prediction did not meet the required precision.

The comparison of calculated and measured critical damage showed a good agreement for the model of effective stresses. Depending on testing conditions, the damage evolution was partly over- or underestimated. These deviations seemed to stem from the usual variations of testing conditions in experiments.

The relation between triaxiality and strain to failure was investigated for various testing conditions. A comparison of collar test and cylindrical specimens at the same temperature showed the influence of triaxiality on the crack initiation. During deformation, an initial positive triaxiality caused specimens to fracture earlier. Temperature variations influence the materials ductility and therefore the crack initiation occurs at lower deformation rates with decreasing temperature.

A semi-empirical grain structure model was linked to the damage model of effective stresses in order to consider the influence of dynamic recrystallization (DRX) on the life

time consumption during hot forming. Both hot compression tests and finite elements simulations were performed and results were compared related to DRX and lifetime consumption. The coupled damage-microstructure model led to retarded lifetime consumption.

EBSD analyses indicated the damage initiation at the grain triple points. For temperatures above the solution temperature of precipitations further ductile crack growth seemed to take place within the DRX grains in a specific direction. At lower temperatures damage was caused by grain boundary fracture. Thus, crack initiation and growth have to be treated separately.

References

[1] P. J. Bolt: Prediction of ductile failure, Eindhoven, 1989 (Ph. D. thesis).
[2] A. S. Wifi, A. Abdel-Hamid, and N. El-Abbasi: J. Mater. Proc. Techn. 77 (1998), p. 285/93.
[3] R. Schiffmann: Experimentelle Bestimmung und modellmäßige Beschreibung der Schädigung beim Gleitbruch von Stahl, 1, Shaker Verlag, Aachen, 2001.
[4] N. Schlüter: Einfluß der Beanspruchung und des Gefüges auf die lokale Schädigung beim Gleitbruch von Baustählen, 1, Shaker Verlag, Aachen, 1996.
[5] Y. Bao and T. Wierzbicki: Trans. ASME 126 (2004), p. 314/24.
[6] M. Rakin, Z. Cvijovic, V. Grabulov, S. Putic, and A. Sedmak: Eng. fract. mech. 71 (2003), p. 813/27.
[7] H. Kim, M. Yamanaka, and T. Altan: Prediction and elimination of ductile fracture in cold forgings using FEM simulations, Proc. NAMRC, 1995, Houghton, Michigan, p. 1/26.
[8] A. M. Freudenthal: The inelastic behaviour of engineering metals and structures, Wiley, New York, 1950.
[9] S. I. Oh, C. C. Chen, S. Kobayashi: Trans. ASME J. Eng. Industry 101 (1979), p. 36/44.
[10] M. G. Cockcroft, D. J. Latham: J. Inst. Metals 96 (1968), p. 33/39.
[11] F. A. McClintock: J. Appl. Mech. 35 (1968), p. 363/71.
[12] J. R. Rice and D. M. Tracey: J. Mech. Phys. Solids 17 (1969), p. 201/17.
[13] M. Oyane: Bulletin JSME 15 (1972), p. 1507/13.
[14] M. Ayada, T. Higashino, and K. Mori: Adv. Techn. Plast. 1 (1984), p. 553/58.
[15] P. Brozzo, B. De Luca, and R. Rendina: A new method for the prediction of the formability limits of metal sheets, Proc. 7th Biennial Congr. of Intern. Deep Drawing Research Group, 1972, p. 3.1/3.5.
[16] D. Zhao, J. P. Bandstra, and H. A. Kuhn: A new criterion for fracture prediction in metalworking processes, Proc. Materials Week, November 2-5 1992, Chicago, Illinois, p. 107/19.
[17] J. Petruška and L. Janiček: J. Mater. Proc. Techn. 80-81 (1998), p. 572/78.
[18] C. Sommitsch and G. Rüf: Ductile fracture analysis with damage models of effective stresses at high temperatures, Proc. 8th Intern. Conf. on Technology of Plasticity, October 9-13, 2005, Verona, Italy.
[19] J. Lemaitre: A Course on Damage Mechanics, 2, Springer Verlag, Berlin, 1996.
[20] U. Prahl, M. Aboutayeb, D. Weichert, U. Achenbach, and X. Wang: Comput. Mater. Sci. 16 (1999), p. 206/12.
[21] F. Andrade Pires, J. Cesar de Sa, L. Costa Sousa, and R. Natal Jorge: Intern. J. Mech. Sci. 45 (2003), p. 273/94.
[22] C. Sommitsch and W. Mitter: Acta Mater. 54 (2006), p. 357/75.
[23] W. Roberts and B. Ahlblom: Acta Metall. 26 (1978), p. 801.
[24] H.-P. Gänser: Intern. J. Plast. 17 (2001), p. 755/72.
[25] S. Gupta, N. Venkata Reddy, and P. M. Dixit: J. Mater. Proc. Techn. 141 (2003), p. 256/65.
[26] C. Sommitsch, M. Walter, S. Kleber, P. Pölt, and S. Mitsche: STEEL GRIPS 3 (2005), p. 287/93.
[27] P. Pölt, C. Sommitsch, S. Mitsche, and M. Walter: Mater. Sci. Eng. A (2006), in press.

Guntram Rüf, MSc
Department of Product Engineering, Materials Center Leoben Forschung GmbH

Dr. Christof Sommitsch
Christian Doppler Laboratory for Materials Modelling and Simulation

Prof. Bruno Buchmayr
Department of Product Engineering

Chair of Metal Forming
University of Leoben, Leoben/Austria